

# Magnetoresistance and magnetization of $\text{La}_{2/3}(\text{Ca}_{0.60}\text{Ba}_{0.40})_{1/3}\text{MnO}_3$ in different temperature ranges<sup>①</sup>

GAI Rong-quan(盖荣权)<sup>1</sup>, HUANG Zhirgao(黄志高)<sup>1, 2</sup>, LAI Heng(赖恒)<sup>1</sup>,  
CHEN Shuiyuan(陈水源)<sup>1</sup>, DU Youwei(都为)<sup>2</sup>

1. Department of Physics, Fujian Normal University, Fuzhou 350007, China;  
2. National Laboratory of Solid State Microstructures, Nanjing University, Nanjing 210093, China

**Abstract:** A polycrystalline  $\text{La}_{2/3}(\text{Ca}_{0.60}\text{Ba}_{0.40})_{1/3}\text{MnO}_3$  was prepared by standard solid reaction method. Magnetization ( $M$ ) and magnetoresistance of the sample were measured between  $T = 77\text{ K}$  and  $350\text{ K}$ . It is found that some correlations exist in the external field dependency of the magnetoresistance magnetoresistance and  $M$  in the low and high temperature regions. Moreover, there are different magnetic field dependence of magnetoresistance and magnetization in different temperature ranges, which indicates the presence of different magnetoresistance mechanisms. Based on the models of spin-polarized tunneling and percolation model, the simulated magnetoresistance obtained using Monte Carlo method well explains the experimental fact.

**Key words:** magnetoresistance; magnetization; manganese perovskite; Monte Carlo method

**CLC number:** O 482.5

**Document code:** A

## 1 INTRODUCTION

The colossal magnetoresistance (CMR) of  $\text{Re}_{1-x}\text{Me}_x\text{MnO}_3$  ( $\text{Re} = \text{La}, \text{Y}$ ,  $\text{Me} = \text{Ca}, \text{Ba}, \text{Sr}, \text{Pb}, \text{K}$ ) with perovskite structure has drawn considerable interest<sup>[1, 2]</sup>. Much theoretical and experimental work has been done to study the physical mechanism of CMR effect. There are two distinct CMR effects in polycrystalline materials: the first one is the low-temperature CMR that increases with decreasing temperature, which is attributed to the spin polarized tunneling through a magnetic barrier in the grain boundaries<sup>[3-12]</sup>. In order to explain the tunneling magnetoresistance of the nano-structured materials, a two-level model of tunneling magnetoresistance containing co-play of the relative orientation of moments between clusters, the intrinsic characters of clusters, Coulomb blockade effect, was suggested in our previous work<sup>[13]</sup>. It is found that the unusual enhancement of magnetoresistance is due to the interaction between the clusters and the intrinsic characters of clusters coating the complex surface. Especially, it is thought that the coating surface of the cluster or the interface between the clusters plays an important role for the enhancement of magnetoresistance. Another one is CMR near the ferromagnetic ordering temperature, which have been explained by several theories, such as percolative phase separation<sup>[14-17]</sup>, the double exchange model with the

Jahn-Teller effect<sup>[18]</sup>, the double exchange model with the non-magnetic disorder<sup>[19]</sup> and the double exchange model with spin-disorder scattering<sup>[20, 21]</sup>. In the percolation model, it is assumed that the sample consists of ferromagnetic metallic particles with a volume fraction randomly distributed over the paramagnetic insulating matrix, and the simulated results suggest that the percolation of FMM domains is responsible for the observed insulator-metal transition<sup>[16]</sup>. The complex magnetic field dependence of magnetoresistance, especially the low-field magnetoresistance (LFMR) and the high-field magnetoresistance (HFMR) at the low-temperature, has also been an interesting topic due to the importance in the understanding of CMR mechanism and applications<sup>[5, 22-24]</sup>. However, up to now, the underlying CMR mechanisms are still unclear. In this paper, the temperature and field dependence of the resistivity and magnetoresistance of polycrystalline sample were studied. Based on the double exchange model with spin-disorder scattering, spin-polarized tunneling effect and Monte Carlo simulation, the magnetoresistances as function of temperature and magnetic field were obtained, which well explain the experimental results.

## 2 EXPERIMENTAL

Polycrystalline sample  $\text{La}_{2/3}(\text{Ca}_{0.60}\text{Ba}_{0.40})_{1/3}\text{MnO}_3$  was fabricated using a standard solid state

① **Foundation item:** Project(G1999064508) supported by the National Key Project for Basic Research of China; Project(E0320002) supported by NSF of Fujian Province of China

**Received date:** 2004-12-06; **Accepted date:** 2005-01-18

**Correspondence:** HUANG Zhirgao, Professor, PhD; Tel: +86-591-83448993; E-mail: zghuang@fjnu.edu.cn

reaction method. The mixed  $\text{La}_2\text{O}_3$ ,  $\text{CaCO}_3$ ,  $\text{BaCO}_3$  and  $\text{MnO}_2$  powers in stoichiometric proportions were ground with an automated mortar at different velocities for 24 h and preheated at 1 000 °C for 10 h. Then they were reground at low velocity for 24 h, pressed into pellets, sintered at 1 290 °C for 24 h. The structures of the materials were analyzed by means of X-ray diffractometry (XRD) with  $\text{Cu K}\alpha$ . Resistivity and magnetoresistance were measured by a standard four-probe in the temperature range of 77–400 K from zero field up to 1.2 T. Magnetization was performed using VSM.

### 3 RESULTS AND DISCUSSION

Fig. 1 shows the magnetization and magnetoresistance as a function of temperature for the sample. From Fig. 1, it is found that magnetoresistance increases evidently with decreasing temperature for  $T < 250$  K, which is attributed to the spin polarized tunneling through a magnetic barrier. A maximum magnetoresistance of 8% is also observed at  $T_p = 295$  K.  $T_p$  is a transition temperature between metal and insulator phases<sup>[1, 2]</sup>. From the thermal magnetization, the Curie temperature of the sample is found to be  $T_c = 303$  K, which is near the value of  $T_p$ . The hysteresis loops of the sample at different temperatures are shown in Fig. 2. It can be seen that, at low temperature as  $T < T_c$  (303 K), a strong ferromagnetic state with small coercivity exists; while at higher temperature as  $T > T_c$ , a linear magnetization curve is found, which means the existence of a paramagnetic state. In order to establish the relation between the magnetoresistance magnitude and magnetization, the formula  $\varphi(M)/\varphi(0) \propto \exp[-c(M/M_s)^2]$  or  $\varphi(M) \propto 1 - M^2$ , has been considered<sup>[20]</sup>. Fig. 3 shows the square of magnetization and magnetoresistance as a function of the external magnetic field at different

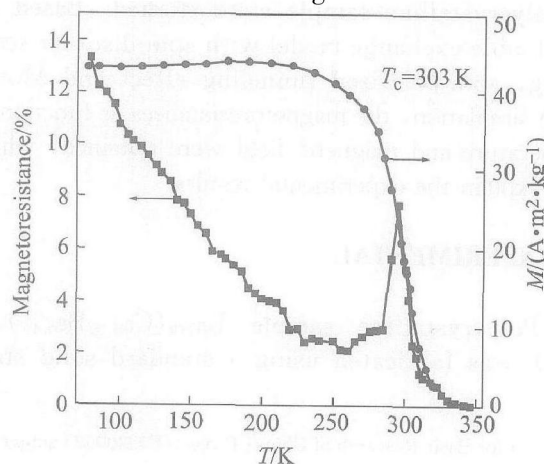


Fig. 1 Magnetization and magnetoresistance as function of temperature for sample

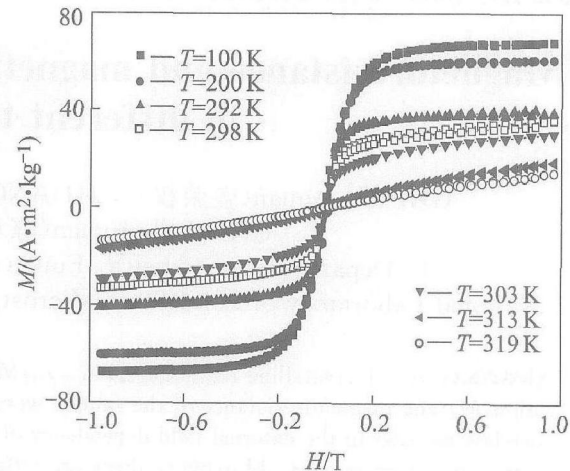
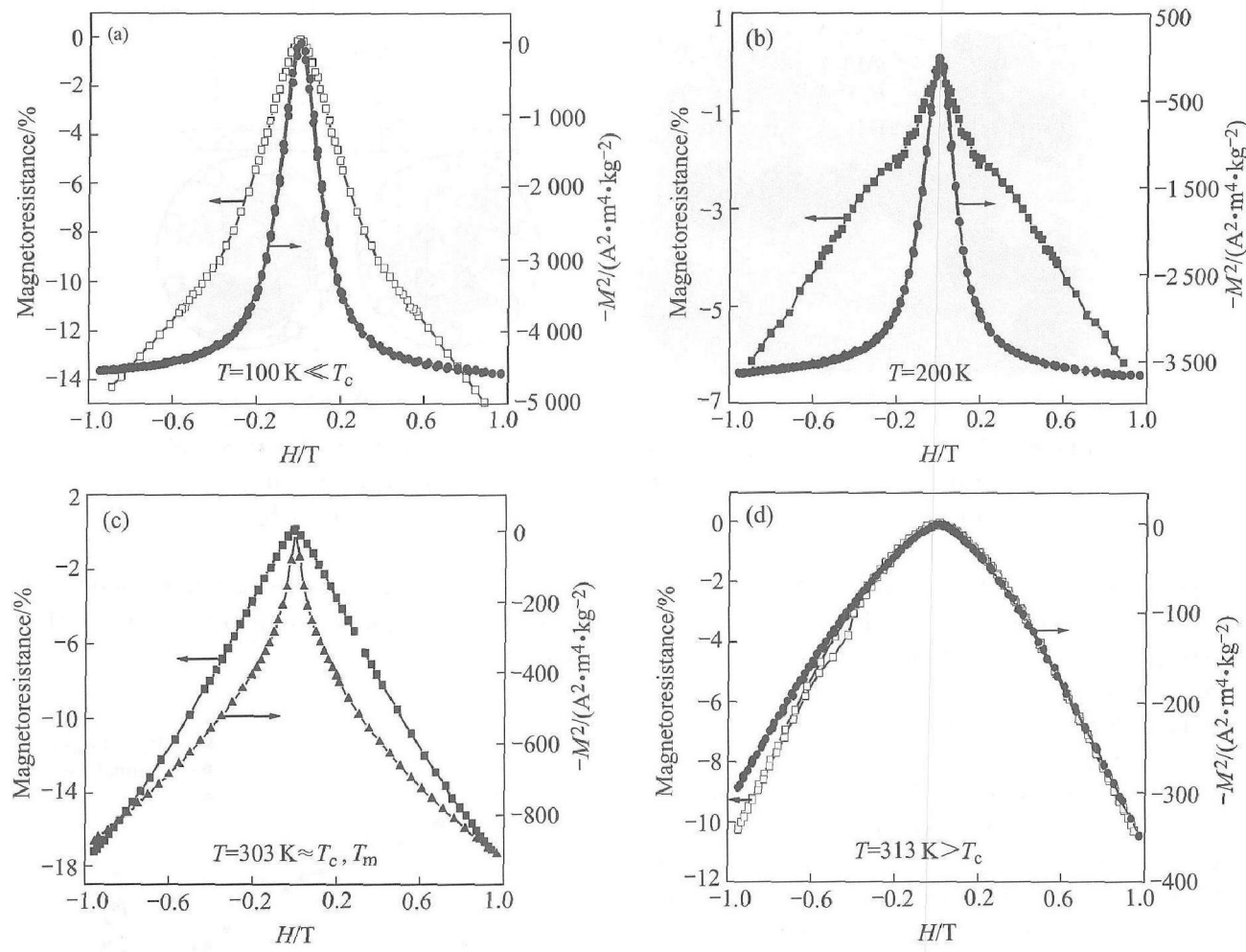


Fig. 2 Hysteresis loops of sample at different temperatures

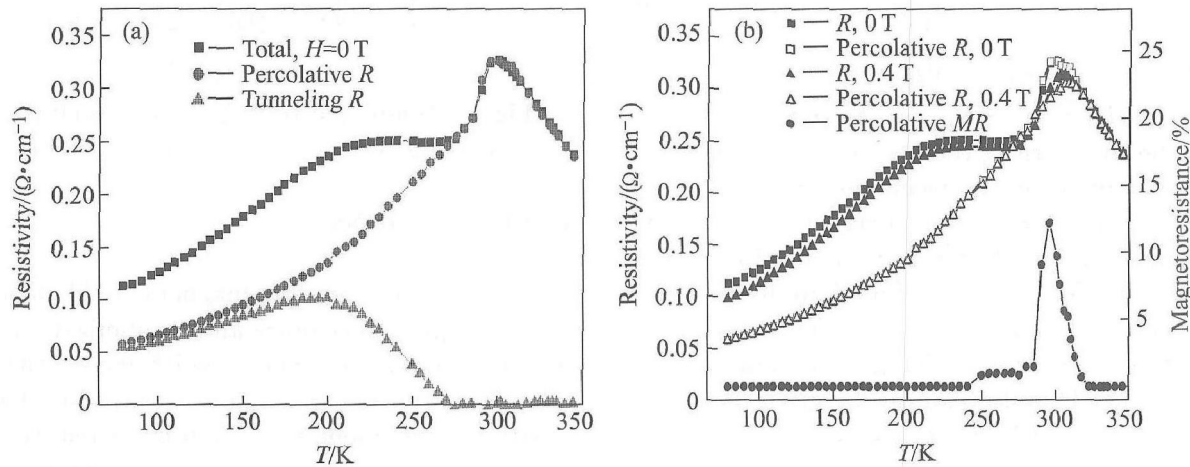
temperatures for  $\text{La}_{0.67}(\text{Ca}_{0.6}\text{Ba}_{0.4})_{0.33}\text{MnO}_3$ . It can be seen that at  $T > T_c$ , magnetoresistance vs  $H$  curve is the same as  $-M^2$  vs  $H$ , which means  $\varphi(M) \propto (1 - M^2)$ . However, as  $T$  is near  $T_c$ ,  $\varphi(M) - H$  curve starts to deviate from the  $M^2$  relation. When  $T$  is below  $T_c$ , the deviation from the  $M^2$  relation becomes more obvious, which means that different magnetoresistance mechanisms may be obeyed in different ranges of temperature. In addition, as temperature is far below  $T_c$ , LFMR and HFMR are observed. It is considered that the LFMR is attributed to the relative orientation of moments between the magnetic clusters, while the HFMR results from the disordered spin scattering in the boundary region.

Fig. 4(a) shows the temperature dependence of the percolative, tunneling and total resistivity with  $H = 0$  for  $\text{La}_{0.67}(\text{Ca}_{0.6}\text{Ba}_{0.4})_{0.33}\text{MnO}_3$  sample. The temperature dependence of the percolative and total resistivity with  $H = 0$ , 0.4 T and the calculated percolative magnetoresistance for  $\text{La}_{0.67}(\text{Ca}_{0.6}\text{Ba}_{0.4})_{0.33}\text{MnO}_3$  sample is shown in Fig. 4(b). Here, the total resistivity is the measured result, and the percolative and tunneling ones are fitted results, which will be discussed in the latter. The double-peak resistivity-temperature ( $\rho$  vs  $T$ ) curve in Fig. 4 is similar to other experimental results<sup>[1–10]</sup>. For the film and single crystalline of manganese perovskite, only single peak is found in  $\rho$  vs  $T$  curves<sup>[3]</sup>.

Based on the recent studies on the tunneling magnetoresistance model in the nanostructured materials<sup>[13]</sup> and percolation model near Curie temperature<sup>[13–16]</sup>, we construct the percolative structure containing ferromagnetic metallic (FMM) clusters and antiferromagnetic (or paramagnetic) insulating (AFI) matrix as seen in Fig. 5(a) and spin tunneling model between the near clusters consisting of complex spin configurations.



**Fig. 3** Magnetoresistance and square of magnetization as function of external magnetic field for  $\text{La}_{0.67}(\text{Ca}_{0.6}\text{Ba}_{0.4})_{0.33}\text{MnO}_3$   
 (a)  $-T = 100\text{ K}$ ; (b)  $-T = 200\text{ K}$ ; (c)  $-T = 303\text{ K} \approx T_c, T_m$ ; (d)  $-T = 313\text{ K} > T_c$



**Fig. 4** Temperature dependence of percolative, tunneling and total resistivity at  $H = 0\text{ T}$  (a), calculated percolative resistivity and magnetoresistance for sample (b)

For a two-phase system (FMM and AFI phases), we can calculate transport properties of compositionally disordered system containing insulators and conductors using percolation theory. It is assumed that the number fraction of FMM clusters is  $p$ . With the similar calculated method in

Ref. [16], we can derive the value of  $p$  from the reduced magnetization curve as seen in Fig. 1. For a  $20 \times 20$  2D lattice with periodic boundary condition, we also can calculate the probability ( $f$ ) in which the system with number fraction ( $p$ ) of FMM clusters is in a conducting state by Monte

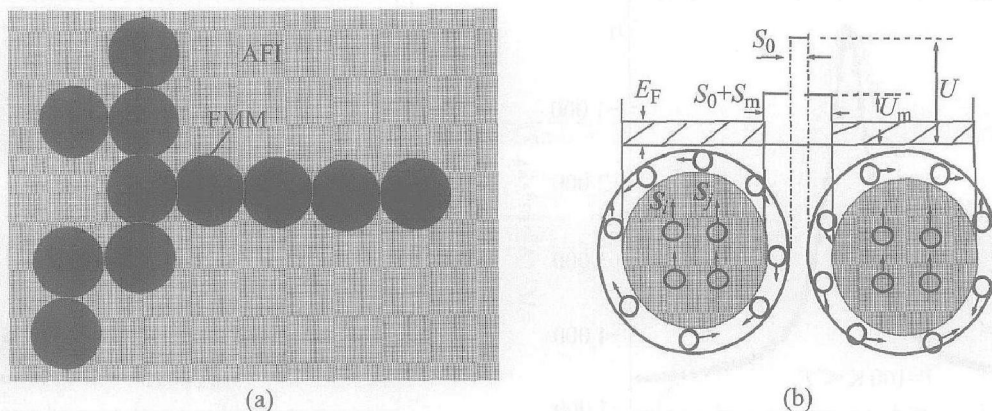


**Fig. 5** Percolative structure containing ferromagnetic metallic clusters and antiferromagnetic (or disordered) insulating matrix(a) and spin-tunneling schematic illustration between near clusters(b)

Carlo simulation. It is assumed that the resistivities of the pure FMM and AFI phases are  $R_M$  and  $R_I$ , respectively. Then the resistivity of the system can be described as:  $R_P = (1-f)R_I + fR_M$ . Here,  $R_I$  corresponds to the Mott's variable range hopping resistivity for  $T > T_c$ <sup>[25]</sup>. From the data of resistivity in Fig. 4, we can get

$$R_I = 5.5 \times 10^{-7} \exp[4.5 \times 10^6 / T]^{1/4} \quad (1)$$

Also, from the best data fitting for the peak of the resistivity in Fig. 4(a), we obtain

$$R_M = 0.00436 + 2.29 \times 10^{-7} T^2 \quad (2)$$

Thus we can get the percolative resistivity at  $H = 0$  and  $0.4 T$ , and the magnetoresistance curve near  $T_c$  can be calculated, as found in Fig. 4(b). Another resistivity coming off the total resistivity is also found in Fig. 4(a), which is thought as the tunneling one.

The tunneling resistivity can be expressed by<sup>[13]</sup>

$$\varrho(H, T) \propto \varrho \cdot \varrho_m = (p - \cos\theta) \cdot \exp(k_0 \sqrt{U_i + \langle \mathbf{S}_{i'} \cdot \mathbf{S}_{j'} \rangle - \langle \mathbf{S}_{i'} \cdot \mathbf{S}_{j'} \rangle}) \quad (3)$$

where the first term  $\varrho$  results from the relative orientation of moments between the magnetic clusters, the second one  $\varrho_m$  is associated with the intrinsic characters of clusters, the definition of the parameters in Eqn. (3) are found in Ref. [13]. Based on the reduced double exchange model with antiferromagnetic superexchange coupling and a magnetic field, Hamiltonian can be given as<sup>[26]</sup>

$$H_{DE} = -T_{DE} \sum_{\langle i, j \rangle} \sqrt{1 + \mathbf{S}_i \cdot \mathbf{S}_j} - J_{AF} \sum_{\langle i, j \rangle} \mathbf{S}_i \cdot \mathbf{S}_j - H \sum_i S_i^z \quad (4)$$

According to Eqns. (3), (4) and combining with Monte Carlo simulation procedure in Ref. [13], we can obtain the temperature dependence of the simulated tunneling magnetoresistance as seen in Fig. 6. Fig. 6 shows the temperature dependence of the simulated percolative, tunneling and total magnetoresistance. Comparing with the results in

Fig. 1, it is found that the simulated ones are consistent with experimental fact, which means that the spin-tunneling and percolative models are quite successful to explain magnetoresistance effect of CMR materials.

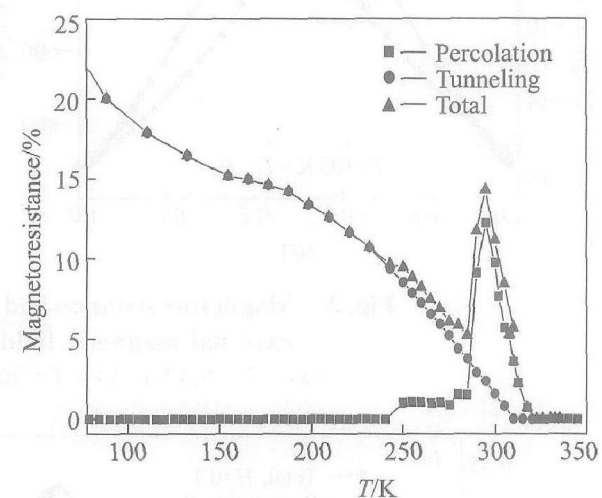


**Fig. 6** Simulated percolative, tunneling and total magnetoresistance as function of temperature

#### 4 CONCLUSIONS

There are different magnetic field dependences of magnetoresistance and magnetization in different temperature ranges, which means the existence of different magnetoresistance mechanism. Based on the models of spin-polarized tunneling and percolation, the simulated magnetoresistance character obtained using Monte Carlo method are consistent with experimental fact, which means that the spin-tunneling and percolative models are quite successful to explain the magnetoresistance effect of the manganese perovskite.

#### REFERENCES

[1] Tokura Y, Tomioka Y. Colossal magnetoresistive

manganites [J]. *J Magn Magn Mater*, 1999, 200: 1–23.

[2] Coey J M D, Viret M, Molnar S V. Mixed-valence manganites [J]. *Adv Phys*, 1999, 48: 167–293.

[3] Gupta A, Gong G Q, XIAO G, et al. Grain-boundary effects on the magnetoresistance properties of perovskite manganite films [J]. *Phys Rev B*, 1996, 54: R15629–5633.

[4] JIANG Y, YUAN S L, HU J F, et al. Evidence of spin-polarized tunneling in phase-separated manganites  $\text{La}_{1/3}\text{Sr}_{2/3-x}\text{Ba}_x\text{MnO}_3$  [J]. *Appl Phys Lett*, 2001, 79: 3470–3473.

[5] Damay F, Cohen L F, Driscoll J M, et al. Low-temperature grain boundaries effect in  $\text{La}_{0.7-x}\text{Y}_x\text{Ca}_{0.3}\text{MnO}_3$  [J]. *J Magn Magn Mater*, 2000, 214: L149–L154.

[6] Ziese M. Grain boundary magnetoresistance in manganites: spin-polarized inelastic tunneling through a spin-glass-like barrier [J]. *Phys Rev B*, 1999, 60: R738–R741.

[7] Mahesh R, Mahendiran R, Raychaudhuri A K, et al. Effect of particle size on the giant magnetoresistance of  $\text{La}_{0.7}\text{Ca}_{0.3}\text{MnO}_3$  [J]. *Appl Phys Lett*, 1996, 68: 2291–2293.

[8] Chechersky V, Nath A, Isaac I, et al. Evidence for breakdown of ferromagnetic order below  $T_c$  in the manganite  $\text{La}_{0.8}\text{Ca}_{0.2}\text{MnO}_3$  [J]. *Phys Rev B*, 1999, 59: 497–502.

[9] Hart C, Hernandez A D, Ares O, et al. Extrinsic magnetoresistance in  $\text{La}_{2/3}\text{Ca}_{1/3}\text{MnO}_3$  thick films [J]. *J Magn Magn Mater*, 2001, 226–230: 905–907.

[10] Steinbeis E, Steenbeck K, Eick T, et al. Epitaxial thin films of magnetic perovskites—preparation, properties and possible applications [J]. *Vacuum*, 2000, 58: 135–148.

[11] Hwang H Y, Cheong S W, Ong N P, et al. Spin-polarized intergrain tunneling in  $\text{La}_{2/3}\text{Sr}_{1/3}\text{MnO}_3$  [J]. *Phys Rev Lett*, 1996, 77: 2041–2044.

[12] Zhang N, DING Weiping, ZHONG Wei, et al. Tunnel-type giant magnetoresistance in the granular perovskite  $\text{La}_{0.85}\text{Sr}_{0.15}\text{MnO}_3$  [J]. *Phys Rev B*, 1997, 56: 8138–8142.

[13] HUANG Zhigao, CHEN Zhigao, PENG Kun, et al. Monte Carlo simulation of tunneling magnetoresistance in nanostructured materials [J]. *Phys Rev B*, 2004, 69: 094420-1–094420-6.

[14] Bastiaansen P J M, Knops H J F. Percolation mechanism for colossal magnetoresistance [J]. *Computational Materials Science*, 1998, 10: 225–229.

[15] Kim H, Dho J, Lee S. Percolative phase separation induced by nonuniformly distributed excess oxygen in low-doped  $\text{La}_{1-x}\text{Ca}_x\text{MnO}_{3-\delta}$  [J]. *Phys Rev B*, 2000, 62: 5674–5677.

[16] Ye S L, Song W H, Dai J M, et al. Large room-temperature magnetoresistance and phase separation in  $\text{La}_{1-x}\text{Na}_x\text{MnO}_3$  with  $0.1 \leq x \leq 0.3$  [J]. *J Appl Phys*, 2001, 90: 2943–2948.

[17] Yuan S L, Li Z Y, Peng G, Xiong C S, et al. Percolation model of the temperature dependence of resistance in doped manganese perovskites [J]. *Appl Phys Lett*, 2001, 79: 90–92.

[18] Millis A J, Littlewood P B, Shraiman B I. Double exchange alone does not explain the resistivity of  $\text{La}_{1-x}\text{Sr}_x\text{MnO}_3$  [J]. *Phys Rev Lett*, 1995, 74: 5144–5147.

[19] Sheng L, Xing D Y, Sheng D N, et al. Metal-insulator transition in the mixed-valence manganites [J]. *Phys Rev B*, 1997, 56: R7053–7056.

[20] Furukawa N. Transport properties of the kondo lattice model in the limit  $S = \infty$  and  $D = \infty$  [J]. *J Phys Soc Jpn*, 1994, 63: 3214–3217.

[21] Yi H, Hong C S, Hur N H. Theoretical considerations on the transport property of  $\text{La}_{1-x}\text{Ca}_x\text{MnO}_3$  in the paramagnetic regime [J]. *Solid State Communications*, 2000, 114: 579–583.

[22] Balcells L, Fontcuberta I, Martinez B, et al. High-field magnetoresistance at interfaces in manganese perovskites [J]. *Phys Rev B*, 1998, 58: R14697–14700.

[23] Rivas J, Hueso L E, Fondado A, et al. Low field magnetoresistance effects in fine particles of  $\text{La}_{0.67}\text{Ca}_{0.33}\text{MnO}_3$  perovskites [J]. *J Magn Magn Mater*, 2000, 221: 57–62.

[24] Markovich V, Rozenberg E, Yuzhelevski, Y et al. Correlation between electroresistance and magnetoresistance in  $\text{La}_{0.82}\text{Ca}_{0.18}\text{MnO}_3$  single crystal [J]. *Appl Phys Lett*, 2001, 78: 3499–3502.

[25] Coey J M D, Viret M, Ranno L, et al. Electron localization in mixed-valence manganites [J]. *Phys Rev Lett*, 1995, 75: 3910–3913.

[26] Tsai S H, Landau D P. Simulation of a classical spin system with competing superexchange and double-exchange interactions [J]. *J Appl Phys*, 2000, 87: 5807–5809.

(Edited by LONG Huai-zhong)